JGR Oceans

RESEARCH ARTICLE
10.1029/2020JC016582

Transports and Accumulations of Greenland Sea Intermediate Waters in the Norwegian Sea

Xiaoyu Wang[1], Jinping Zhao[1,2], Tore Hattermann[3], Long Lin[4], and Ping Chen[5]

[1]Frontiers Science Center for Deep Ocean Multispheres and Earth SystemKey, Laboratory of Physical Oceanography, Ocean University of China, Qingdao, China, [2]College of Oceanic and Atmospheric Sciences, Ocean University of China, Qingdao, China, [3]Norwegian Polar Institute, Tromso, Norway, [4]Second Institute of Oceanography, Ministry of Natural Resources, Hangzhou, China, [5]National Engineering and Technological Research Center of Marine Monitoring Equipment, Institute of Oceanographic Instrmentation, Qilu University of Technology (Shandong Academy of Sciences), Qingdao, China

Key Points:

- We examine water masses transported from the Greenland Sea to the Norwegian Sea using hydrographic data collected in 2015
- A gap in the Mohn Ridge acted as a major passage of intermediate waters when the outflow in the Jan Mayen Channel was temporarily ceased
- Atlantic-origin Water becomes an important component of the Greenland Sea intermediate waters to feed the Iceland-Scotland Overflow Water

Correspondence to:
X. Wang,
wangxiaoyu331@163.com

Citation:
Wang, X., Zhao, J., Hattermann, T., Lin, L., & Chen, P. (2021). Transports and accumulations of Greenland Sea intermediate waters in the Norwegian Sea. *Journal of Geophysical Research: Oceans*, *126*, e2020JC016582. https://doi.org/10.1029/2020JC016582

Received 7 JUL 2020
Accepted 17 MAR 2021

Abstract The Greenland Sea intermediate waters transported via the Jan Mayen Channel (JMCh) are a significant source for the Iceland-Scotland Overflow Water. Based on hydrographic data collected by a Norway-China survey in 2015 and Argo floats, we classify the water masses of the Greenland Sea outflow and then reveal their distributions in the Norwegian Sea. The Atlantic-origin water produced by density increase during winter in the northern Greenland Sea was an important component of the intermediate waters exported to the Norwegian Sea, accounting for about 30% of the total volume in 2015. The hydrographic data revealed that the major passage of outflow from the Greenland Sea was located in the southern Mohn Ridge in 2015, rather than in the JMCh, as generally recognized. The transport of intermediate waters from the Greenland Sea via the southern Mohn Ridge in the summer of 2015 is estimated to be about 0.8–1.7 Sv. This transport pattern provides a perspective that there exists a multi-passage system of outflow in the JMCh and Mohn Ridge, promoting a stable supply of intermediate waters to the Norwegian Sea.

Plain Language Summary The Arctic Intermediate Water produced by open-ocean convection in the Greenland Sea Gyre is known as a major source of the deepest overflow across the Iceland-Scotland Ridge. We reveal that the Atlantic-origin water densified in the northern Greenland Sea was another important source of overflow, which was associated with the increasing component of the Atlantic Water in the Greenland Sea. These different sources of overflow waters in the Greenland Sea indicate an underestimate of water production if only the Greenland Sea Gyre is considered. Our study also indicates that the Mohn Ridge can have an equivalent contribution as the Jan Mayen Channel in terms of feeding the Iceland-Scotland Overflow Water.

1. Introduction

The Nordic Seas include the Greenland Sea, Iceland Sea, and Norwegian Sea, with a total area of approximately 2.5×10^6 km^2. The principal basin-wide boundary circulation in the Nordic Seas is cyclonic, with the Norwegian Atlantic Current on the east and the East Greenland Current on the west (Hansen & Østerhus, 2000; Rossby et al., 2009; Swift & Aagaard, 1981; Voet et al., 2010). The Jan Mayen Ridge, the Jan Mayen Fracture Zone, and the Mohn Ridge divide the Nordic Seas into four unique basins: the Greenland Basin, the Lofoten Basin, the Norwegian Basin, and the Iceland Plateau (Figure 1).

One important role of the Nordic Seas in the climate system is to provide overflows that maintain the lower limb of the Atlantic Meridional Overturning Circulation (Chafik & Rossby, 2019; García-Ibáñez et al., 2018; Hansen & Østerhus, 2000; Våge et al., 2015). Observations show that both the Denmark Strait Overflow Water (DSOW) and Iceland-Scotland Overflow Water (ISOW) have the same densities of 27.8–28.06 kg/m^3 (Hansen & Østerhus, 2000; Köhl, 2010). The DSOW is thought to be mainly supplied by the East Greenland Current, which carries the Arctic-origin and Atlantic-origin waters to the Denmark Strait (Harden et al., 2016; Mastropole et al., 2017; Rudels et al., 2002). However, some studies argued that the North Icelandic Jet can make an equal contribution to the DSOW (Pickart et al., 2017; Våge et al., 2011, 2015). A new study indicated that the densest portion of the DSOW largely originates in the Greenland Sea Gyre (Huang

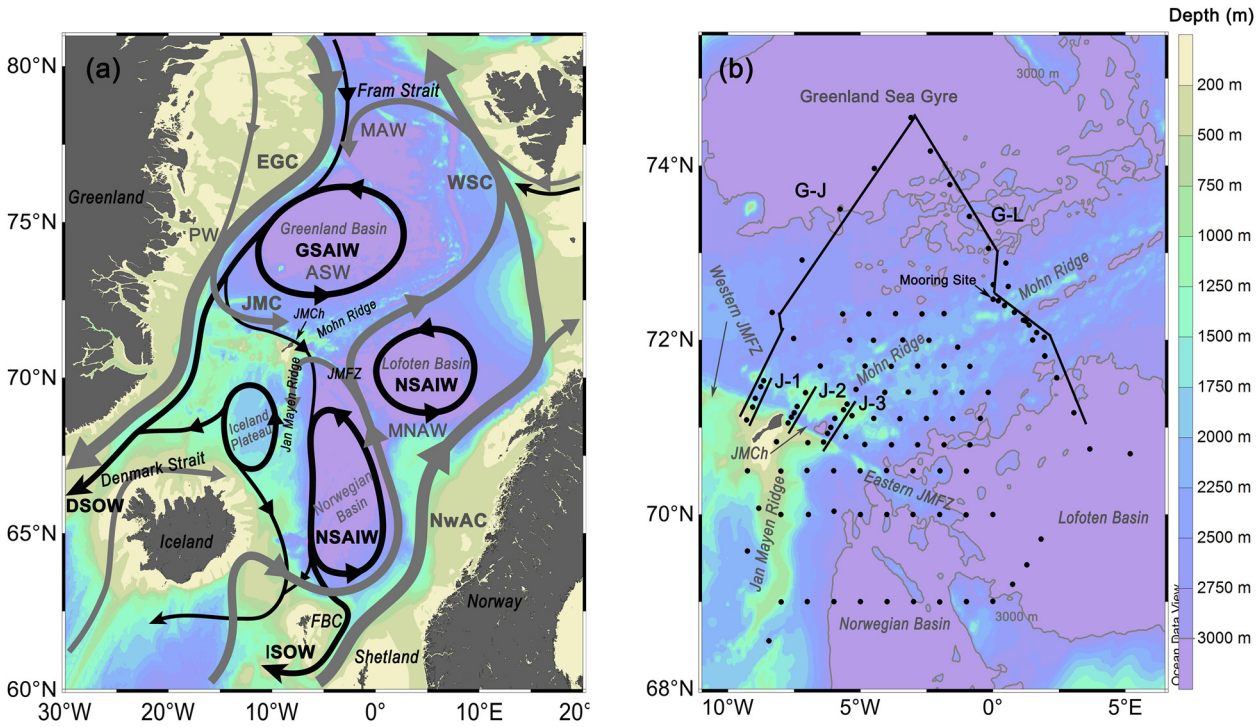

Figure 1. (a) Schematic diagram of the circulation in the Nordic Seas (based on Hawker [2005]). (b) Black dots are the CTD stations sampled during the joint Norway-China cruise. Black lines mark sections G–J, G–L, J-1, J-2, and J-3, respectively. ASW, Arctic Surface Water; CTD, conductivity, temperature, and depth; DSOW, Denmark Strait Overflow Water; EGC, East Greenland Current; FBC, Faroe Bank Channel; GSAIW, Greenland Sea Arctic Intermediate Water; ISOW, Iceland-Scotland Overflow Water; JMC, Jan Mayen Current; JMCh, Jan Mayen Channel; JMFZ, Jan Mayen Fracture Zone; MAW, Modified Atlantic Water; MNAW, Modified Norwegian Sea Atlantic Water; NSAIW, Norwegian Sea Arctic Intermediate Water; NwAC, Norwegian Atlantic Current; PW, Polar Water; WSC, West Spitsbergen Current.

et al., 2020). As for the ISOW in the Faroe Bank Channel (FBC), the lower portion with densities of 28.00–28.07 kg/m^3 is mainly supplied by the Norwegian Sea Arctic Intermediate Water (NSAIW) and Norwegian Sea Deep Water (Harden et al., 2016), which are mainly from the Greenland Sea (Eldevik et al., 2009; Huang et al., 2020; Shao et al., 2019). The upper portion with densities of 27.8–28.0 kg/m^3 is mainly supplied by the Norwegian Atlantic Water (MNAW) from the Norwegian Sea and by the East Icelandic Water from the Iceland Sea (Eldevik et al., 2009; Hansen & Østerhus, 2000; Mckenna and Berx, 2016). The upper boundary of the Norwegian Sea Deep Water has become deeper than 1,400 m in the Norwegian Sea since the early 1990s (Latarius & Quadfasel, 2016; Turrell et al., 1999), which is associated with the cessation of deep convection in the Greenland Sea (Budéus et al., 1998; Lauvset et al., 2018; Moore et al., 2015). The 28.06 kg/m^3 isopycnal to the north of the FBC also deepens to a depth close to 1,000 m (Semper et al., 2020), which is much deeper than the sill depth of 850 m in the FBC. The vertical change of water mass distribution means that currently waters denser than 28.06 kg/m^3 in the southern Norwegian Basin can only make a minor contribution to the ISOW (Turrell et al., 1999), even counting the upward diapycnal mixing associated with the mixing-driven secondary boundary circulation (Somavilla, 2019; Visbeck & Rhein, 2000). Thus, the Greenland Sea intermediate waters of most concern are those with densities of 27.97–28.06 kg/m^3, which play a major role in feeding the ISOW.

For the Greenland Sea intermediate waters (27.97–28.06 kg/m^3), the dominant water mass is Greenland Sea Arctic Intermediate Water (GSAIW), which is the main product of open-ocean convection (Jeansson et al., 2008; Karstensen et al., 2005; Schott et al., 1993). The seasonal production of the GSAIW in the Greenland Sea Gyre has exceeded 1.0 Sv (1 Sv = 10^6 m^3/s) on average (Brakstad et al., 2019). Considering that the mean winter mixed layer depth beyond the gyre is about half of that within the gyre, the overall production of newly ventilated intermediate waters in the Greenland Sea is probably larger than 1.5 Sv. Generally, the GSAIW supplies the overflow via two pathways (Figure 1): one along the eastern continental slope of Greenland to feed the DSOW, and the other via the Jan Mayen Channel (JMCh) and then along the interior

circulation of the Norwegian Sea (Eldevik et al., 2009; Olsson et al., 2005). Transport of the GSAIW via the Denmark Strait is estimated to be as large as 0.5 Sv based on long-term observations (de Steur et al., 2014; Mastropole et al., 2017; Våge et al., 2013). This means the other pathway should provide a volume transport larger than 1.0 Sv. However, the observed outflow via the JMCh was unstable and even reversed at times (Østerhus & Gammelsrød, 1999). Thus, there must exist other passages to compensate for the intermittent shut-off in the JMCh. A complex multi-passage outflow system, which consists of the JMCh and numerous gaps in the mid-ocean ridge, is suggested by chemical tracer data (Olsson et al., 2005). However, the topography around Jan Mayen is fairly rugged. Topography-enhanced turbulent mixing causes strong modification of water masses, and induces large uncertainties about the outflow structure. So far, detail on water mass transport from the Greenland Sea through the Jan Mayen-Mohn Ridge is still lacking.

In addition to the GSAIW, the Atlantic Water (AW) can also become denser than 27.97 kg/m^3 due to cooling around the Fram Strait (Hattermann et al., 2016; Marnela et al., 2016; Schlichtholz & Houssais, 1999). Although the volume flux of the AW into the Nordic Seas remains stable in the past decades (Østerhus et al., 2019), the northward transports of heat and salt have increased significantly (Lauvset et al., 2018; Merchel & Walczowski, 2020; Mork et al., 2014), indicating a greater influence of the AW on water properties in the Nordic Seas. It has been well studied that the Atlantic-origin water (including the AW and its modifications) plays an important role in supplying the overflow via the Denmark Strait (de Steur et al., 2014; Håvik et al., 2017; Mastropole et al., 2017). Also, part of the Atlantic-origin water is carried by the Jan Mayen Current to the southern Greenland Sea (Bourke et al., 1992). However, the pathways of the Atlantic-origin water being exported to the Norwegian Sea are still unclear, not to mention its influences on the overflows.

In the summer of 2015, a high-resolution (~30 km spacing) survey using an array consisting of 120 stations was conducted in the central Nordic Seas. This high-resolution array consisting of nine zonal sections was designed to present a detailed outflow structure from the Greenland Sea. It provides a great opportunity to investigate water transport around Jan Mayen. Using these hydrographic data, we seek a comprehensive understanding of water transport from the Greenland Sea into the Norwegian Sea. We investigated (1) composition of water masses in the intermediate layer of the Greenland Sea, (2) accumulation of exported Greenland Sea intermediate waters in the Norwegian Sea, and (3) detail of water transports via the JMCh and across the Mohn Ridge.

2. Data and Methods

2.1. Hydrographical Data

A joint Norway-China oceanographic cruise was conducted in June 2015, sampling 120 stations in the central Nordic Seas (Figure 1b). Hydrographic casts were collected by a Sea-bird 25 plus conductivity, temperature, and depth (CTD) sensor on the Norwegian vessel R/V Stålbas. The sensor was calibrated at the Sea-bird facilities in Seattle before and after the cruise. The CTD casts were processed according to the Sea-bird processing procedures with temperature and salinity accuracies of 0.001°C and 0.003°C, respectively.

Section G–L, which extended from the Lofoten Basin to the Greenland Basin, was visited two times over a 14-day interval on June 2 and June 16. Section G-J started from the Greenland Sea Gyre on June 4 and ended at the western Jan Mayen Ridge 1 day later. Three short sections, which are located at the upstream, midstream, and downstream of the JMCh, respectively (J1, J2, and J3 shown in Figure 1b), were observed during June 5–6. From June 8 to 16, a hydrographic array was conducted within the fractured zone east of the JMCh. A mooring array equipped with four Aanderaa current meters was deployed at depths of 250, 600, 1,000, and 1,450 m at the Mohn Ridge (0.0°W, 72.5°N; Station M04). All the current meters operated from June 5 to 19, with a configuration of 5-min sampling interval. The manufacturer estimates for the Doppler Current Sensor accuracies are ±0.15 cm/s for current speed, ±5° for current direction, and ±3° for magnetic compass. The current direction was corrected according to the magnetic declination provided by the National Centers of Environmental Information, NOAA (https://www.ngdc.noaa.gov/geomag/magfield.shtml).

Table 1
Water Mass Classification in the Central Nordic Seas

Water mass	Acronym	Water mass boundary			Characteristics in θ-S diagram
		θ (°C)	S	σ (kg/m^3)	
Polar Water	PW	$\theta < 0$	$S < 34.40$	$\sigma_\theta < 27.7$	Arctic origin, including the polar mixed layer and halocline.
Modified Norwegian Atlantic Water	MNAW	$1 < \theta < 12$	$34.80 < S < 35.15$	$27.40 < \sigma_\theta < 27.97$	Maximum in both temperature and salinity.
Arctic Surface Water	ASW	$0 < \theta < 2$	$34.70 < S < 34.90$	$\sigma_\theta < 27.97$	Distributed in summer surface mixed layer, highly affected by solar radiation and freshwater input. Obvious seasonal variations in temperature, salinity, and density.
Modified Atlantic Water	MAW	$0 < \theta < 1$	$S < 34.92$	$\sigma_\theta > 27.97$, $\sigma_\theta < 28.02$	Scattered along the mixing line of the Atlantic Water and PW or winter water with near-freezing temperature. Slope in the θ-S diagram is positive.
dense Atlantic Water	dAW	$0 < \theta < 2$	$S > 34.92$	$\sigma_\theta > 28.02$, $\sigma_\theta < 28.05$	Denser than the MAW at the same salinity level. Slope in the θ-S diagram is positive.
Greenland Sea Arctic Intermediate Water	GSAIW	$-1 < \theta < 0$	$34.80 < S < 34.92$	$27.97 < \sigma_\theta$, $\sigma_\theta < 28.06$, $\sigma_{0.5} < 30.44$	Upper S and θ decreasing with depth, while lower S and θ increasing with depth. It is typically identified as a cold, low-salinity layer above the Arctic Ocean deep water in the Greenland Sea.
Norwegian Sea Arctic Intermediate Water	NSAIW	$-0.5 < \theta < 0.5$	$34.87 < S < 34.91$	$27.97 < \sigma_\theta$, $\sigma_{0.5} < 30.44$	A salinity minimum layer under the MNAW in the Norwegian Sea.

2.2. Water Mass in θ-S Diagram

In the upper layer, the Polar Water (PW) from the Arctic Ocean is generally trapped on the eastern shelf of Greenland, and the Arctic Surface Water (ASW) dominates in the Greenland Basin (Bourke et al., 1987; Hawker, 2005; Rudels et al., 2002). Along the Mohn Ridge, the ASW meets the MNAW, which is the dominant water mass in the upper layer of the Norwegian Sea (Orvik & Niiler, 2002), and forms the Arctic Front. The property of the MNAW has large ranges in both temperature and salinity due to different modification processes (Kostianoy & Nihoul, 2009; Latarius & Quadfasel, 2016; Richards & Straneo, 2015). Detailed salinity and temperature ranges of each water mass and its brief description are given in Table 1.

The GSAIW produced by open-ocean convection is the densest intermediate water in the Nordic Seas (Langehaug & Falck, 2012; Marnela et al., 2016); thus, it shapes the basic pattern of density dome in the region (Aagaard et al., 1985). The Atlantic-origin water recirculating southward from the vicinity of the Fram Strait is another important intermediate water in the Nordic Seas (Hattermann et al., 2016; Rudels et al, 2005, 2008). It can be further divided into two subtypes, the Modified Atlantic Water (MAW) and dense Atlantic Water (dAW) (Marnela et al., 2008, 2013): The MAW is a mixture of the AW with relatively fresh and cold waters, such as the PW and GSAIW (Boyd & D'Asaro, 1994; Hattermann et al., 2016; Schlichtholz & Houssais, 2002), while the dAW is a production of surface cooling and densification of the MNAW along its way to the Fram Strait in winter (Marnela et al., 2008, 2013), which is similar to the formation of the GSAIW. The dAW is also called "colder Atlantic Water" (Schlichtholz & Houssais, 1999). The property differences between the MAW and dAW, which are related to different formation processes, shown in θ-S diagram (Figures 2e and 2f). Figure 2f shows that the MAW distributes along the mixing line of the MNAW and GSAIW, while the dAW is a bit denser and distributes between 28.02 and 28.04 kg/m^3 isopycnals with maximum in both temperature and salinity.

A relatively low-salinity structure also exists in the intermediate layer of the Norwegian Sea, where the water mass is called the NSAIW. Unlike the GSAIW, the NSAIW is a mixture of intermediate waters that originated in the Greenland Sea and Iceland Sea (Blindheim & Rey, 2004; Eldevik et al., 2009; Jeansson et al., 2017). The NSAIW is recognized as a major contributor to the ISOW with a 40%–60% composition (Bringedal et al., 2018; Fogelqvist et al., 2003; McKenna et al., 2016; Turrell et al., 1999).

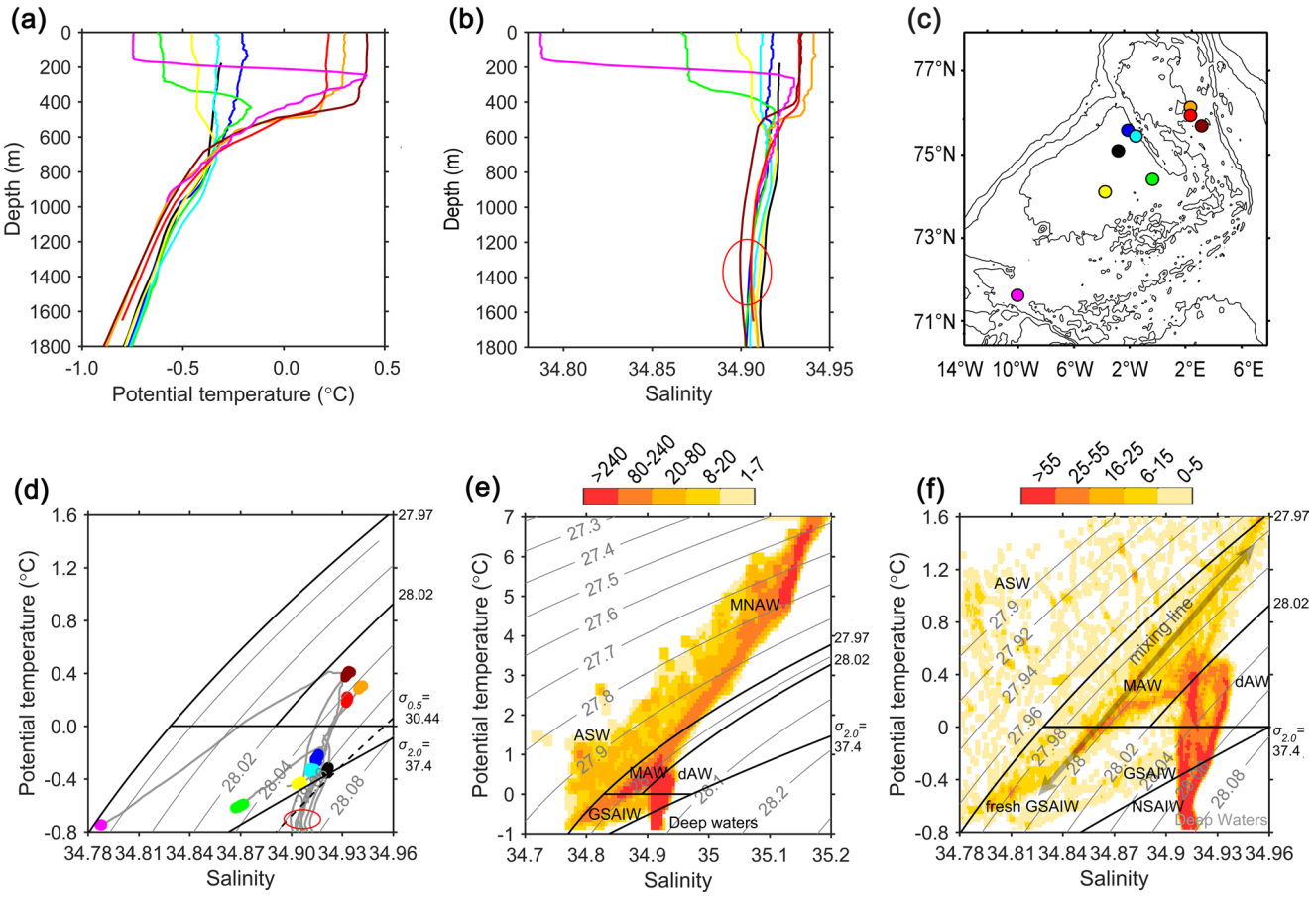

Figure 2. Profiles of (a) potential temperature and (b) salinity when open-ocean convection reached the deepest from February to April 2015. (c) The locations of corresponding Argo floats are shown in matching colors. (d) θ-S diagram of the mixed-layer waters during the period from February to April 2015. (e) θ-S diagram of the CTD profiles collected by the joint Norway-China cruise. Shading represents the number of scatters in each area unit. (f) Detailed illustration of water masses in θ-S diagram. The salinity minimum layer at a depth deeper than 1,500 m in (b and d) is indicated by a red circle. CTD, conductivity, temperature, and depth.

2.3. Argo Data and Winter Water Mass Property

The hydrographic profiles captured by Argo floats from February to June 2015 are used to obtain the properties of winter mixed-layer water after open-ocean convection in the Greenland Sea (71°N–77°N). The Argo data downloaded from the archives of the International Argo Program had been calibrated before being released (Good et al., 2013). Considering the small salinity differences inside the central gyre, we used a data quality control by comparing the Argo data with the hydrographic data during the same period to exclude slight salinity drift. The layer chosen to make this comparison was the salinity minimum at the depth deeper than 1,500 m (shown in Figures 2b and 2d). The structure of salinity minimum in this layer makes the water mass there easy to be accurately identified. Moreover, the salinity of deep water is more stable than that of shallow water. When the salinity difference between the Argo sampling and neighboring CTD sampling was less than 0.01, the Argo float itself was considered to be of good quality. Eventually, 9 floats were selected from all 11 Argo floats in spring 2015. In Figure 2, we only show the profiles of each float when the mixed layer reached its maximum depth. Thus, the properties of winter mixed layer water in Figure 2d approximately represent the densest state that the newly produced GSAIW could achieve in 2015.

Continued warming and salinification of the Greenland Sea in recent years have been noted by many researchers (Jeansson et al., 2017; Karstensen et al., 2005; Lauvset et al., 2018; Wang et al., 2015). These changes are mainly due to the increasing input of heat and salt by the northward AW (Holliday et al., 2008; Yashayaev & Seidov, 2015). Also, the density of the GSAIW inside the Greenland Sea Gyre has been decreasing since the 1990s due to the warming during winter that weakens the capacity of water densification

(Brakstad et al., 2019; Moore et al., 2015). This indicates that the criterion of $\sigma_{0.5} = 30.44$ kg/m^3 (referenced to 500 dbar), which was adopted about 20 years ago to distinguish the GSIAW (Rudels et al., 2002), may bring inaccuracy if recently collected data are used. For instance, part of the deep water would now be included in the newly produced GSIAW if we use the previous criterion ($\sigma_{0.5} = 30.44$ kg/m^3) (Figure 2d). Thus, according to the maximum density of the GSAIW in 2015 (yellow, blue, black, and bright blue dots), a new criterion of $\sigma_{2.0} = 37.40$ kg/m^3 (referenced to 2,000 dbar) is adopted in this study to identify the lower boundary of the newly produced GSAIW. Obviously, the deviation of the GSAIW from $\sigma_{2.0} = 37.40$ kg/m^3 is significantly smaller than that from $\sigma_{0.5} = 30.44$ kg/m^3. Note that the new criterion may not be applicable for situations in other years.

In the southern Greenland Sea close to Jan Mayen, water in the mixed layer was much lighter and fresher, with a density less than 28.02 kg/m^3 and salinity lower than 34.8 (pink contour in Figure 2) than the water further north. Considering that this relatively fresh water belonged to the intermediate layer and was also produced by open-ocean convection, it should be classified as a subtype of the GSAIW. We call it fresh GSAIW ($S < 34.85$, σ_θ: 27.97–28.02 kg/m^3) to differentiate it from the GSAIW (σ_θ: 28.02–28.06 kg/m^3) originated in the central gyre. Once exported to the Norwegian Sea, these two subtypes of GSAIWs with different density ranges would penetrate into different depths, both feeding the overflows.

Moreover, in the northern Greenland Sea close to the West Spitsbergen Current, the dominant water in the winter mixed layer was the dAW, with a thickness of nearly 500 m (dark red, red, and orange dots). The density of the dAW ($\theta > 0$°C, $S > 34.93$) was less than that of the GSAIW within the gyre, but it was denser than the fresh GSAIW in the southern basin.

3. Transport and Accumulation of Greenland Sea Intermediate Waters in the Norwegian Sea

3.1. Distribution of Intermediate Waters Across the Greenland Sea in 2015

Although the layer within the Greenland Sea Gyre from the surface to 350 m was fully occupied by the GSAIW after winter open-ocean convection (Figure 2), observations in the subsequent summer revealed that the GSAIW in the upper layer (<350 m) had been completely replaced by less dense waters such as the ASW and MAW (Figure 3). However, the lower boundary of the GSAIW, that is, the isocline of $\sigma_{2.0} = 37.40$ kg/m^3, was still maintained at a depth of about 900–1,000 m, which was the same as that in the previous winter. This indicates that the reduction of the GSAIW was due to self-export from the central gyre rather than sinking to a deeper depth.

Beyond the gyre, the intermediate waters arriving at the southern Greenland Sea (south of 73.5°N), including the fresh GSAIW, dAW, and GSAIW. The fresh GSAIW existed only in the subsurface layer between 50- and 200-m depths, which was the maximum depth reached in 2015 by the regional shallow convection in the southern Greenland Sea. The dAW was found in a layer between 250- and 600-m depths, causing both a temperature maximum and a salinity maximum in the vertical direction (Figures 3b and 3d). The ring-like distribution of the dAW along the boundary indicates that it was transported into the southern Greenland Sea by the cyclonic boundary current system consisting of the East Greenland Current and Jan Mayen Current. The dAW had a larger distribution within the boundary current about 150 km wide and 300 m thick. According to the mean area percentages of different water masses in G–J and G–L, which could be obtained using their property ranges in Table 1, the dAW accounted for about 30% of the total volume of the Greenland Sea intermediate layer. Although we have only 1-year measurements, our data suggest that, at least in 2015, the dAW was an important component of the Greenland Sea intermediate waters. In a deeper layer of depths 600–900 m, the lower portion of the GSAIW ($\sigma_\theta > 28.05$ kg/m^3, $\sigma_{2.0} < 37.40$ kg/m^3) was also observed from the central gyre to the Greenland Sea boundary near the Mohn Ridge (Figure 3). It even formed a high-salinity core at 1,000–1,200 m in the western boundary of the Norwegian Sea (~72°N in section G–L, Figure 3d), suggesting an export from the Greenland Sea. Details of this transport process are presented in Sections 3.2 and 3.3.

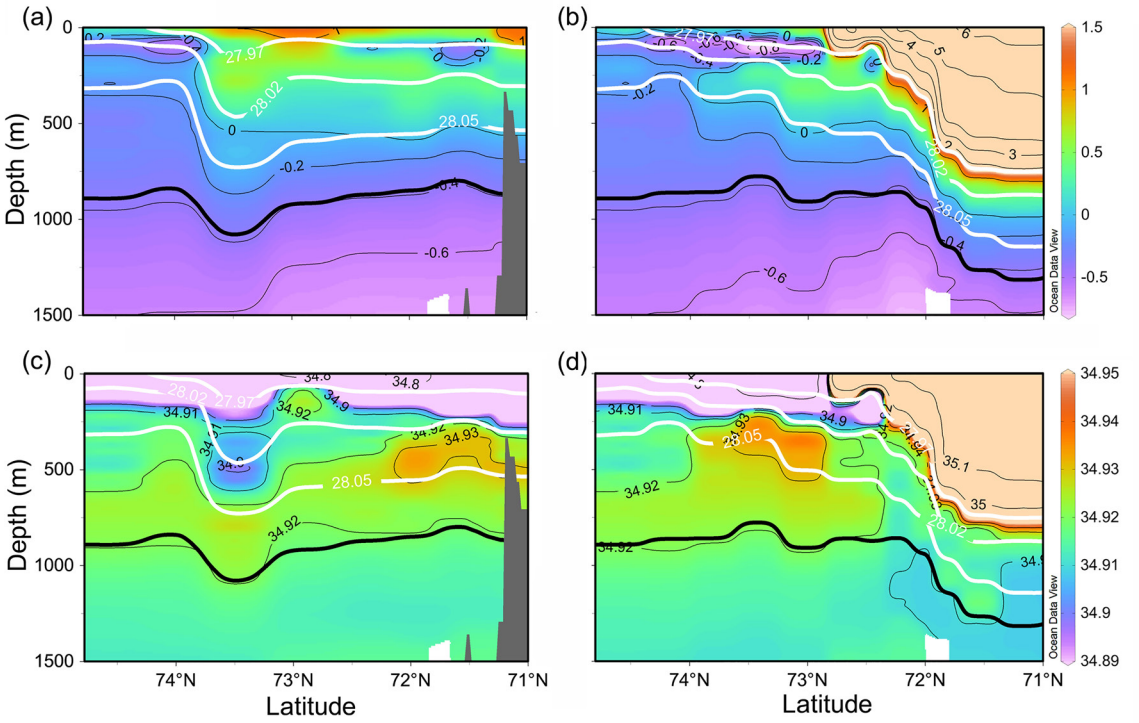

Figure 3. (a) Potential temperature and (c) salinity along section G–J, extending from the central Greenland Sea Gyre to the West Jan Mayen Fracture. (b) Potential temperature and (d) salinity distributions along section G–L, extending across the Mohn Ridge from the Greenland Sea on the left, eastward to the Norwegian Sea on the right. Three white contours represent isopycnals of 27.97, 28.02, and 28.05 kg/m^3, respectively; and the thick black contour is $\sigma_{2.0}$ = 37.40 kg/m^3.

3.2. Distributions of the Greenland Sea Intermediate Waters in the Norwegian Sea

Here, for each exported intermediate water, we use its median density as a targeted tracer interface to track its distribution in the Norwegian Sea. For the fresh GSAIW, its median density was about 27.99 kg/m^3 (Figure 2f). After being exported, the fresh GSAIW was gradually modified by mixing with the warm and saline MNAW, leading to a relatively fresh and cold mixed water ($0 < \theta < 1$°C, $S < 34.93$) along the eastern Jan Mayen Fracture Zone and Jan Mayen Ridge (Figures 4a–4c). The distribution of this mixed water was no deeper than 350 m in the Norwegian Sea, contributing only to the shallow part of the ISOW.

For the dAW, the median density of its high-salinity core ($S > 34.92$) was about 28.035 kg/m^3 (Figure 2f). Figures 4d and 4e show the exported dAW with two branches as a warm and high-salinity tongue extending along the cyclonic intermediate circulation in the Norwegian Basin and Lofoten Basin. In the northern Norwegian Basin (69.5°N–71°N), the dAW occupied a layer at 300–650 m, close to the Jan Mayen Ridge with its southward branch acting as a source of heat and salt for the ISOW downstream. At the same time, the other branch of the dAW in the Lofoten Basin distributed in a layer deeper than 1,000 m (Figure 4f), which was too deep to directly take part in the overflows.

For the GSAIW, $\sigma_{2.0}$ = 37.385 kg/m^3 was chosen as the targeted interface to trace its distribution. Figures 4g–4i show that the exported GSAIW was located at 700–850 m, taking part in forming the deepest part of the ISOW. The GSAIW also became a source of heat and salt in the intermediate layer of the Norwegian Sea, as the dAW did. It seems that the "Atlantification" argued by Polyakov et al. (2017) not only took place in the Arctic Ocean, but also occurred in the Nordic Seas. Evidently, the Greenland Sea is the place where the heat and salt start to transfer from the surface into the deep ocean before being transported southward, implying its important role in the global heat budget.

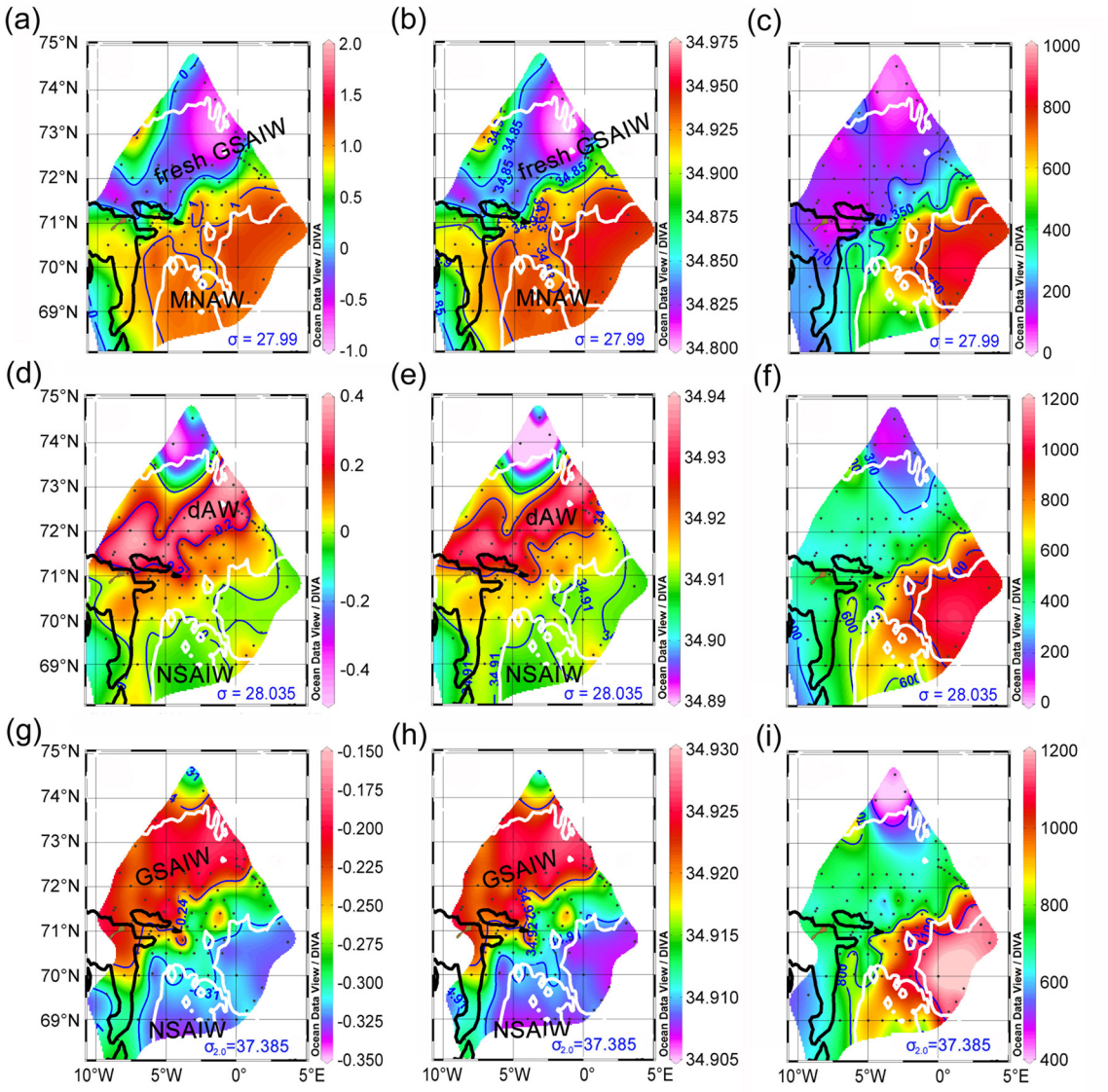

Figure 4. Distributions of (a) potential temperature, (b) salinity, and (c) depth on $\sigma_\theta = 27.99$ kg/m^3. (d–f) are the same as (a–c), respectively, except on $\sigma_\theta = 28.035$ kg/m^3; (g–i), on $\sigma_{2.0} = 37.385$ kg/m^3. The thick black and white contours mark water depths of 1,500 and 3,000 m, respectively.

3.3. Transport of Intermediate Waters Across the Mohn Ridge

The mooring deployed on the northwest side of the Mohn Ridge in section G–L (0.0°W, 72.5°N) recorded a mean speed of 8.1 cm/s toward the Mohn Ridge at a depth of 250 m (Figure 5). Comparison of the first and repeated measurements (Figures 6a–6d) along section G–L shows that the fresh GSAIW was transported about 100 km eastward to the Mohn Ridge over a 14-day period. The mean speed estimated from these two measurements was about 7.8 cm/s, similar to the mooring records. The transport of the fresh GSAIW across the Mohn Ridge was in the manner of subduction, approximately along the isopycnals of 27.97–28.02 kg/m^3 (Figures 6a–6d). The fresh GSAIW was gradually modified into the MAW by mixing with the MNAW within the Arctic Front when being subducted into the Norwegian Sea, which could be inferred from the properties of several microscale low-salinity cells (i.e., the core of the fresh GSAIW) along the mixing line in θ-S diagram (Figure 2f). After being exported, the fresh GSAIW occupied the layer between 300- and 500-m depths at the western boundary of the Norwegian Sea in the form of the MAW. Note that the MAW in the Norwegian Sea is formed by the regional mixing of the fresh GSAIW and MANW, which is different from that originated along the western Greenland Sea. Having a high proportion of the fresh GSAIW, the MAW

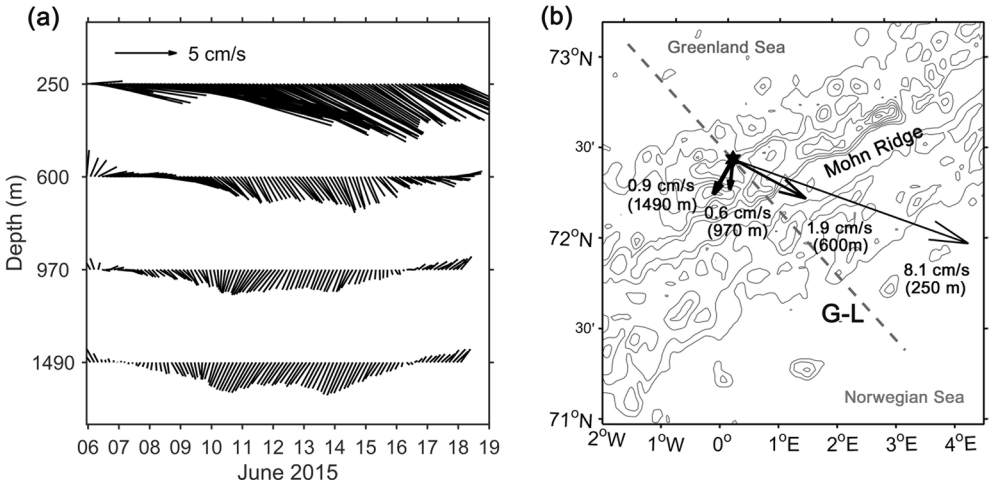

Figure 5. Observed (a) velocity and (b) mean currents during the 14-day period.

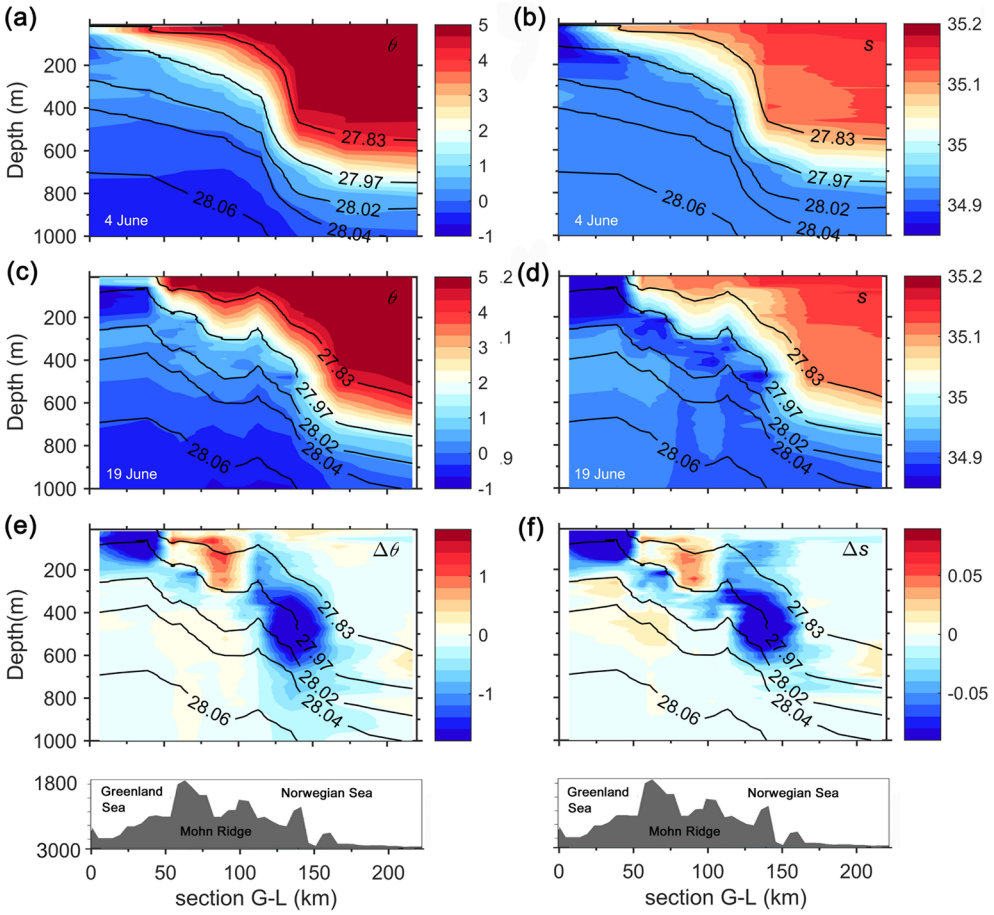

Figure 6. Hydrographic distributions along section G–L, which was visited two times during the survey. (a) Potential temperature and (b) salinity during the first visit on June 4. Panels (c and d) show the potential temperature and salinity, respectively, from the second visit on June 19. The differences in (e) potential temperature and (f) salinity between the two visits 15 days apart. Topography along the section is shown in the bottom panels.

was relatively colder and fresher than the MNAW in the Norwegian Sea, resulting in the observed decreases in temperature and salinity (Figures 6e and 6f).

The dAW (28.02–28.05 kg/m^3) in depths of 250–550 m beneath the fresh GSAIW was also observed to be transported eastward. The mooring recorded a mean speed of about 1.9 cm/s at a depth of 600 m. Considering the baroclinicity of flow close to the ocean front, the actual mean speed of the dAW exported from the Greenland Sea was probably between 1.9 and 8.1 cm/s. The dAW transport from the Greenland Sea brought extra heat and salt to the Norwegian Sea. The net eastward transport of the GSAIW in the lower intermediate layer was relatively weak, being only 0.6 cm/s.

Although the Greenland Sea intermediate waters were observed to be transported across the Mohn Ridge, the exact mechanism determining the export is not yet clear. Uncertainties mainly exist in two aspects. First, the export might be a synoptic process related to wind-induced adjustment to cyclonic activities. However, our mooring measurements are not long enough to record the velocity changes under plenty of cyclones. Second, the Mohn Ridge is much longer than what we covered during the survey. At present, we have no way to evaluate the whole volume transport of the outflows, nor can we calculate the corresponding heat or salt transport.

3.4. Water Mass Transport in the Jan May Channel

Of the three sections in the JMCh (J-1, J-2, and J-3 in Figure 7a), both J-1 and J-2 showed similar hydrographic structures as those in section G–J (Figure 3). This consistency indicates that the Greenland Sea intermediate waters indeed entered the JMCh. However, J-3, which was located at the eastern end of the channel, apparently showed different distributions of water masses. The fresh GSAIW ($\theta < 0$°C) in the subsurface layer tended to absent at J-3. In the meanwhile, the dAW ($\theta > 0$ °C, $S > 34.92$) was significantly diminished; only a lower portion remained (can only be identified by the isohaline of 34.92 deeper than 500 m). Considering the sill depths at the south side of the JMCh between J-2 and J-3 are only 250–500 m, it was impossible for the dAW to be completely exported from the channel by crossing the sill southward before arriving at J-3. Moreover, the fresh GSAIW and dAW had already existed in the vicinity of the JMCh during winter (see the pink contour in Figure 2), indicating that seasonal variation also could not explain the observed hydrographic difference among J-1, J-2, and J-3. Geostrophic velocity (zonal component) calculated with a reference level of 1,500 m gives a diagnostic perspective to infer the cause. At J-3, an east-to-west flow occurred, intruding into the JMCh along its northern boundary (Figure 7j). In the meantime, a narrow west-to-east flow occurred at J-2 in the southern boundary close to the sill of the Jan Mayen Fracture Zone. However, it seems that the eastward outflow could not originate in the Greenland Sea due to the fact that the outflow at J-1, which was upstream of J-2, was not only weaker but also shallower (Figure 7h). This jet-like narrow flow at J-2 was probably related to the westward water intrusion from J-3 to J-2, which forced waters inside the channel to come out. Thus, the weak and shallow outflow at J-1 suggests that water exchange between the Greenland Sea and Norwegian Sea via the JMCh was significantly weakened at least during the period of the cruise. Due to the lack of long-term current monitoring in the JMCh, we cannot reveal the duration or frequency of the blocking, nor can we identify the mechanism causing the weakening of water exchange. To gain deeper understanding, more observations are needed.

The Mohn Ridge has numerous steep ridges and gaps. At its southern end (5°W, 71.3°N; Figure 8a), close to the JMCh, there exists a huge gap about 50-km wide and 2,000-m deep. We call this gap the Mohn Ridge Channel (MRCh).

As shown in Figures 8b and 8c, a massive amount of the Greenland Sea intermediate waters was being exported through the MRCh. Both the fresh GSAIW and dAW in the MRCh kept their original properties in the Greenland Sea well. For instance, the dAW in section G–J (Figure 3c) and in the MRCh (Figure 8c) had almost the same high-salinity core ($S > 34.93$). For comparison, only waters with salinities of 34.92–34.93 could be found in the JMCh, indicating the limited distribution of the dAW there. This result suggests that the outflow via the MRCh was significantly stronger than that in the JMCh. The other evidence to support this finding comes from the trajectory of an Argo float with a parking depth of 950 m. The float changed its path from the JMCh toward the MRCh on May 23, 2015, and then passed the MRCh on October 5 **(**Figure 8a**)**. Although the parking depth of the float was a bit deeper than the layer where the dAW was, the

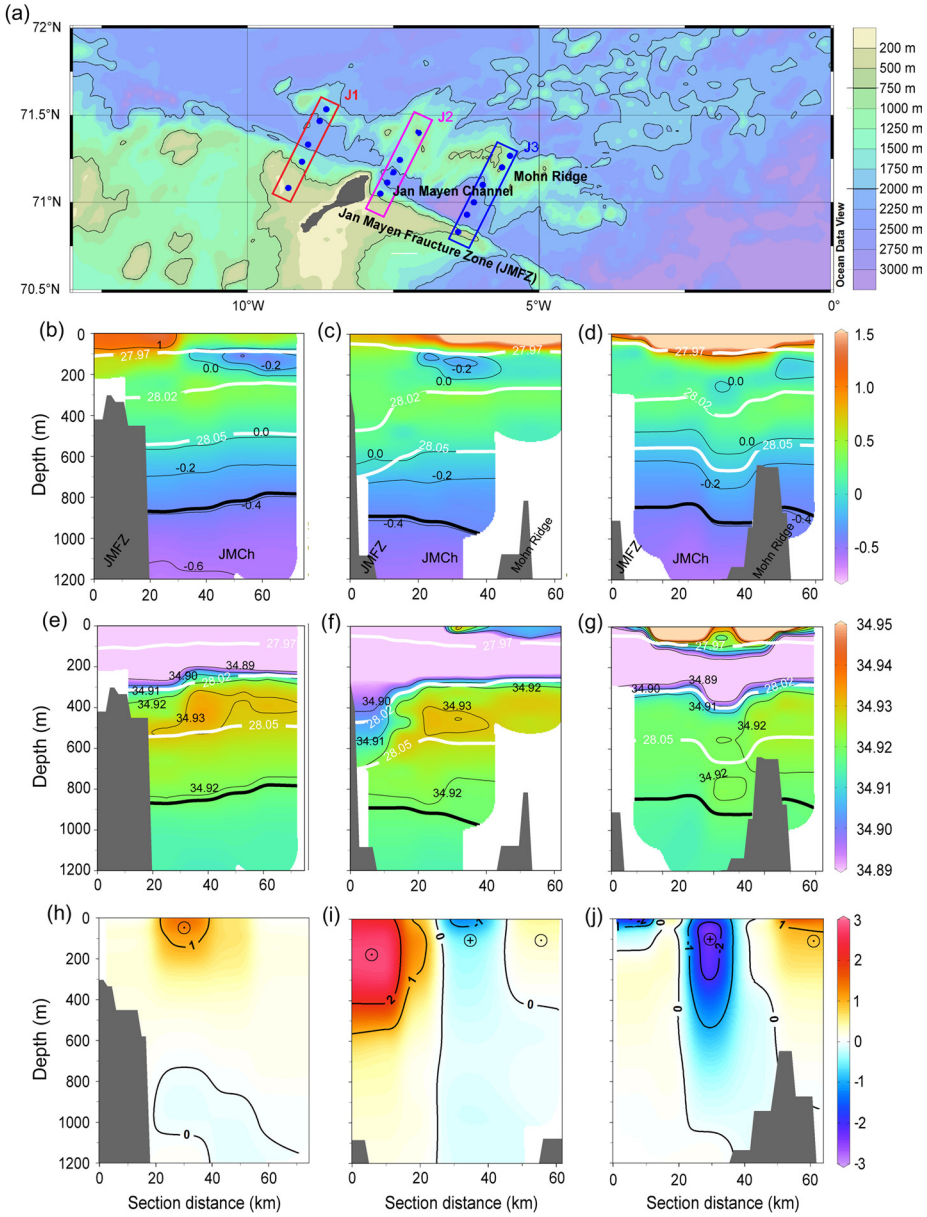

Figure 7. (a) Locations of sections J-1, J-2, and J-3 in the JMCh. Potential temperature distributions are shown in (b) J-1, (c) J-2, and (d) J-3; and salinity distributions in (e) J-1, (f) J-2, and (g) J-3. Geostrophic flow structures are shown in (h) J-1, (i) J-2, and (j) J-3. Three white contours represent isopycnals of 27.97, 28.02, and 28.05 kg/m^3, respectively; and the thick black contour is $\sigma_{2.0} = 37.40$ kg/m^3.

change of its trajectory still indicates that the MRCh was a major passage of intermediate outflow from the Greenland Sea. In addition, the straight drift of the float toward the MRCh suggests that the outflow via the MRCh probably lasted longer than 3 months.

4. Discussion

The MRCh and JMCh are nearly the same in terms of width and depth. It seems that the MRCh acts as a major passage of the outflow from the Greenland Sea in the case when the JMCh is temporarily blocked. A mean speed of about 2.0 cm/s in the MRCh was estimated based on the drift of the Argo float, which was a bit faster than the mooring recorded 0.6 cm/s at a depth of 970 m. This difference was reasonable considering the wider and deeper topography in the MRCh, which benefits an outflow regionally induced by

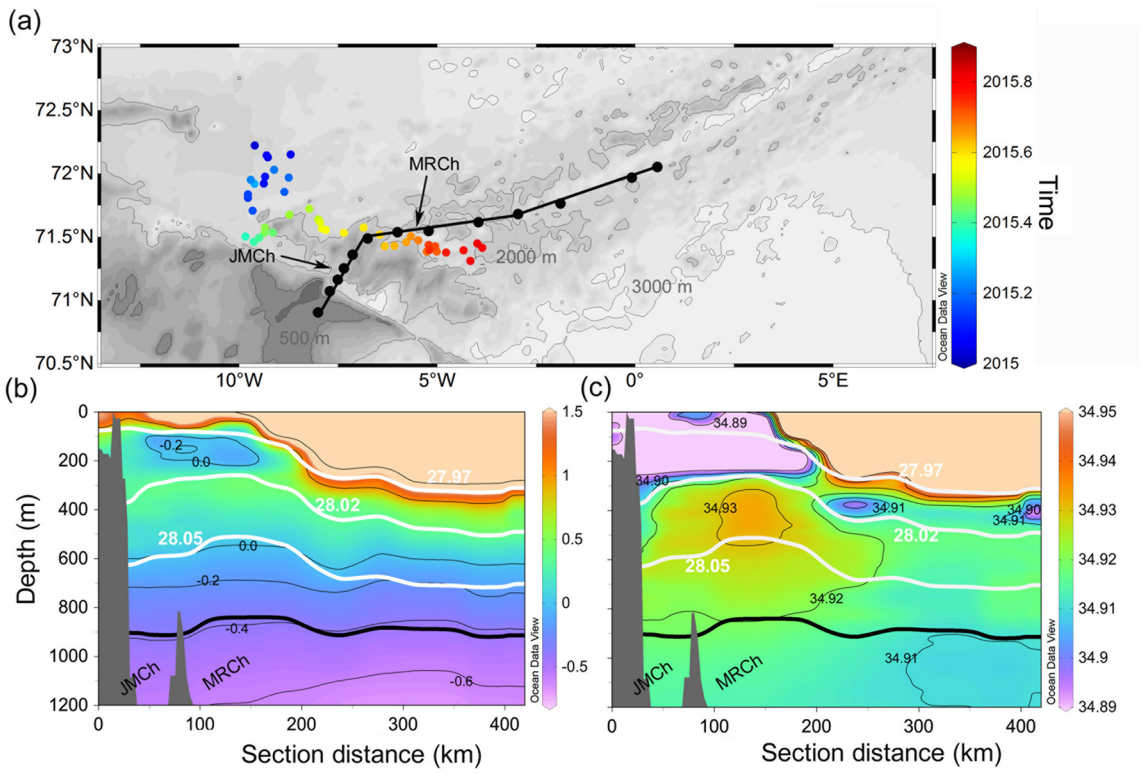

Figure 8. (a) Locations of hydrographic stations along the Mohn Ridge. Balck dots mark the hydrographic stations, and colored dots mark the locations of the Argo floats. Distributions of (b) potential temperature and (c) salinity along the Mohn Ridge. Three white contours represent isopycnals of 27.97, 28.02, and 28.05 kg/m^3, respectively; and the thick black contour is $\sigma_{2.0}$ = 37.40 kg/m^3.

potential vorticity. Thus, the volume transport of the Greenland Sea intermediate waters (27.97–28.06 kg/m^3) through the MRCh was estimated to be about 0.8 Sv on the assumption of a width of 50 km and a speed of 2.0 cm/s. Actually, the speed of the upper part of the outflow was probably larger than 2.0 cm/s due to the baroclinicity observed by the mooring, leading to an actual transport larger than 0.8 Sv. If we take into account the vertical velocity structure as shown by the mooring records in Figure 5b, the transport in the MRCh can reach ~1.7 Sv, which is sufficient to explain the huge seasonal output of intermediate waters within the Greenland Sea.

The estimated volume transport via the MRCh in the summer of 2015 was equivalent to the transport of about 0.5–1.6 Sv via the JMCh estimated by previous studies (Hawker, 2005; Shao et al., 2019; Swift & Koltermann, 1988). Thus, we suggest that there should exist a multi-passage system in the Jan Mayen-Mohn Ridge for the Greenland Sea intermediate waters that are transported into the Norwegian Sea. The newly identified passage in the MRCh should be viewed as an important part of the multi-passage system to maintain a stable supply of overflow waters.

Our observation results reveal that the supply of intermediate waters via the MRCh was even equivalent to that in the JMCh. However, limited by sparse and discontinuous observations, the mechanism driving the outflow is still unclear. With the help of a high-resolution coupled ocean model, better understanding with more detailed information is expected.

The ISOW is basically comprised of two types of waters, the Atlantic Water and Arctic Intermediate Water. The former is warm (2°C–4°C) and is recognized to be involved in the overflow around the Iceland-Shetland Ridge. The latter is cold (<0°C) and is recognized to be produced by open-ocean convection in the Iceland Sea and Greenland Sea. Only the Greenland Sea intermediate waters are dense enough (>28.02 kg/m^3) to feed the lower portion of the ISOW (Huang et al., 2020; Semper et al., 2020). In the past, when deep convection prevailed in the Greenland Sea, the intermediate waters were even below −1°C (Brakstad et al., 2019).

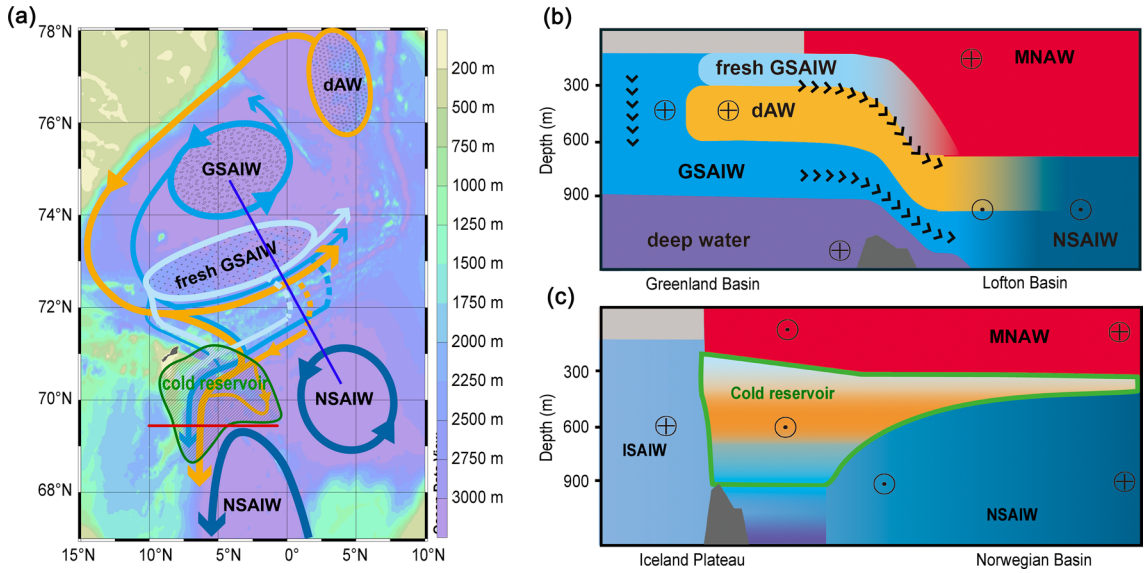

Figure 9. (a) Schematic of the transports of Greenland Sea intermediate waters. The coverage of the cold reservoir is marked by a green contour. (b) Vertical structure of water masses from the section marked in blue in (a). (c) Vertical structure of water masses from the section marked in red in (a).

Shao et al. (2019) used the term "cold reservoir" for the intermediate waters that originated in the Greenland Sea and accumulated in the Norwegian Sea. Although the temperature of the exported waters has increased to about −0.7°C–0.4°C (Figures 4a–4g) due to the continuous warming in the Greenland Sea in the past few decades, they are still much colder than the MNAW (2°C–4°C). It has been known that open-ocean convection in the Greenland Sea provides the largest geopotential in the Nordic Seas, leading to a dome-like density structure. The cold reservoir, which is formed by the exported intermediate waters from the "density dome" in the Greenland Sea, also acts as a high geopotential source in the Norwegian Sea, causing a geopotential structure of "high in the north, low in the south." Without the cold reservoir, the intermediate layer of the Norwegian Basin would be occupied by waters from the Iceland Sea completely, where the geopotential is lower than that in the Greenland Sea. The cold reservoir piles up in the northern Norwegian Basin once being exported from numerous passages among the JMCh and Mohn Ridge. However, its accumulation mechanism is still not clear. We speculate that it might be associated with ocean dynamics in the southern Norwegian Basin, for example, water exchange with the Iceland Sea, or wind-stress condition over the southern Nordic Seas. More studies are needed to answer this question.

We present a schematic of the sources and distributions of water masses that made up the cold reservoir based on the hydrographic data in 2015 (Figure 9). In winter, the geopotential in the Greenland Sea Gyre increased greatly due to sufficient open-water convection. In the meantime, the Ekman pumping caused by positive wind stress curl in the Greenland Sea caused a high sea surface height around the boundary, which balanced the increased geopotential. With the weakening of the wind stress curl in spring and summer, the GSAIW (σ_θ > 28.05 kg/m^3) inside the gyre will be exported to the boundary under the forcing of gravity. After being transported into the Norwegian Sea via the passages in the JMCh and Mohn Ridge, the GSAIW occupied the depth range of 650–850 m along the western boundary of the Norwegian Sea (blue arrows). At the same time, the dAW, which was produced by the densification of the MNAW in the northern Greenland Sea, occupied the layer of 300–650 m (yellow arrow). Note that the dAW had been partly modified by mixing with the GSAIW during its long-distance advection along the boundary of the Greenland Sea. Compared with the dAW and GSAIW, the fresh GSAIW had a much narrower distribution. Only a small portion can be traced to the layer between 250 and 350 m.

As the northernmost ice-free deep ocean in the Northern Hemisphere, the hydrographic conditions in the Greenland Sea are sensitive to high-latitude climate change. Thus, the cold reservoir, which consists of waters from the Greenland Sea, can be regarded as an intermediate conveyor belt transferring the signals of climate change to the overflow in terms of water mass transport. Our results reveal heat and salt transports

from Greenland to the intermediate layer of the Norwegian Sea via the cold reservoir, which had direct effects on the properties of the ISOW. Then, the heat and salt are further transferred to the deep Atlantic Ocean via the overflows, as argued by Chen and Tung (2014, 2018) and Hansen et al. (2016).

We also observed a deeper branch of the Greenland Sea intermediate waters in the Lofoten Basin. Voet et al. (2010) pointed out that the intermediate circulation in the Lofoten Basin was cyclonic and few floats could drift southward along the Norwegian slope. Thus, this deeper branch seemed to have a long journey to reach the FBC and feed the ISOW there. In addition, a small portion of the waters in the branch could be transported northward into the Greenland Sea and Arctic Ocean by joining the West Spitsbergen Current. However, we could not provide more details of this deeper branch due to the lack of data.

The mean depth of the 28.06 kg/m^3 isopycnal in the Norwegian Basin has deepened from about 1,000 m to about 1,200 m in the past 10 years, whereas the 27.97 kg/m^3 isopycnal remains unchanged (Latarius & Quadfasel, 2016). This changing trend indicates that the supply of intermediate waters (27.97–28.06 kg/m^3) for overflows is still sufficient if we ignore any changes in flow speed. Is it possible that this is partly related to the increased portion of the dAW in the intermediate layer as a result of "Atlantification" over the years? And to what extent could the Atlantic-origin water compensate for the density deficit caused by the continuous warming in the Nordic Seas? To answer these questions, more observations and high-resolution ocean simulations are needed.

5. Conclusions

Using the hydrographic data obtained in the Nordic Seas in the summer of 2015, we studied water transport via the JMCh-Mohn Ridge and its subsequent accumulation in the Norwegian Sea. The main conclusions are as follows:

1. The dAW ($0 < \theta < 2$°C, $S > 34.92$, $28.02 < \sigma_\theta < 28.05$ kg/m^3) densified in the northern Greenland Sea in 2015 became an important component of the Greenland Sea intermediate waters, accounting for about 30% in volume. It was transported to the eastern Greenland Sea by the boundary current and occupied a layer between 200 and 500 m, forming a maximum in both temperature and salinity. Together with the GSAIW ($\theta < 0$°C, $34.90 < S < 34.92$, $\sigma_{2.0} \sim 37.40$ kg/m^3), which was produced in the Greenland Sea Gyre, these two water masses made up the main body of the Greenland Sea intermediate waters. In addition, the fresh GSAIW ($\theta < 0$°C, $S < 34.85$, $27.97 < \sigma_\theta < 28.02$ kg/m^3) as the main production of shallow convection in the southern Greenland Sea occupied a layer no deeper than 200 m. All three intermediate waters were observed to be exported into the Norwegian Sea, indicating that the contribution of the Greenland Sea waters to the ISOW is significantly underestimated if only the Greenland Sea Gyre is considered.
2. After being exported into the Norwegian Sea, the Greenland Sea intermediate waters accumulated along the mid-ocean ridge, forming a cold reservoir with a considerable volume in the intermediate layer, which eventually was transported southward and took part in feeding the ISOW. Apart from contributing to the overflow, another deeper branch is identified stretching toward the Norwegian slope. However, this west-to-east branch entrained by the cyclonic circulation in the Lofoten Basin was too deep to have a direct effect on the properties of the ISOW. It might take part in the renewal of intermediate and deep waters of the Nordic Seas and Arctic Ocean.
3. Using the data from a repeated hydrographic section combined with mooring data, we captured a synoptic process of water mass export across the Mohn Ridge in 2015. The transport of the Greenland Sea intermediate waters into the Norwegian Sea was dominantly along isopycnals. The fresh GSAIW, with a mean speed of about 8.1 cm/s, gradually sank to a depth of 200–500 m at the western boundary of the Norwegian Sea. Beneath it, the dAW and GSAIW, with speeds of 1.9 and 0.6 cm/s, respectively, were also transported across the Mohn Ridge, causing increases in temperature and salinity due to their properties being warmer and more saline than the pre-existing NSAIW.
4. The hydrographic data collected in 2015 reveal an important passage in the Mohn Ridge for the Greenland Sea intermediate waters being exported to the Norwegian Sea. The estimated volume flux in the channel was about 0.8–1.7 Sv, implying its role in feeding the overflow as important as the JMCh. Thus, we argue that there exists a multi-passage system between the JMCh and Mohn Ridge, which probably promotes a stable exchange of intermediate waters. For the situation in 2015 when the JMCh was

temporarily blocked, the channel in the Mohn Ridge acted as a major passage to feed the NSAIW. However, in a longer perspective, there still remain some unsolved questions about the multi-passage system, for example, how often the JMCh is blocked, if there are some seasonal (or shorter or longer) variability within the system, and how about the northern part of the Mohn Ridge? These questions need to be addressed with observational and modeling studies in the future.

Data Availability Statement

The hydrographic data analyzed in this study can be obtained from the Chinese National Arctic and Antarctic Data Center (https://www.chinare.org.cn/en/metadata/0465d918-8de7-427f-ba6d-48e94fd351ad) or from the Zenodo (a general-purpose open-access repository operated by the European Organization for Nuclear Research, https://doi.org/10.5281/zenodo.4571352). Argo data are downloaded from the International Argo Program (http://www.argo.ucsd.edu/Gridded_fields.html). Some figures shown in this paper were illustrated using the Ocean Data View software (Schlitzer, Reiner, Ocean Data View, https://odv.awi.de, 2020).

Acknowledgments
This study is funded by the Chinese Natural Science Foundation (Grant nos. 41976022 and 41606212) and the National Key R&D Program of China (Grant no. 2019YFA0607001). The authors thank the crew on the Norwegian R/V Stålbas for their assistance and hard work. The authors also thank the members from Shanghai Ocean University who participated in the cruise and contributed to the fieldwork. Support from Akvaplan-niva is highly appreciated (https://www.akvaplan.niva.no/).

References

Aagaard, K., Swift, J. H., & Carmack, E. C. (1985). Thermohaline circulation in the Arctic Mediterranean seas. *Journal of Geophysical Research*, *90*(C3), 4833–4846. https://doi.org/10.1029/JC090iC03p04833

Blindheim, J., & Rey, F. (2004). Water-mass formation and distribution in the Nordic Seas during the 1990s. *ICES Journal of Marine Science*, *61*(5), 846–863. https://doi.org/10.1016/j.icesjms.2004.05.003

Bourke, R. H., Newton, J. L., Paquette, R. G., & Tunnicliffe, M. D. (1987). Circulation and water masses of the East Greenland shelf. *Journal of Geophysical Research*, *92*(C7), 6729–6740. https://doi.org/10.1029/JC092iC07p06729

Bourke, R. H., Paquette, R. G., & Blythe, R. F. (1992). The Jan Mayen Current of the Greenland Sea. *Journal of Geophysical Research*, *97*(C5), 7241–7250. https://doi.org/10.1029/92JC00150

Boyd, T. J., & D'Asaro, E. A. (1994). Cooling of the West Spitsbergen Current: Wintertime observations west of Svalbard. *Journal of Geophysical Research*, *99*(C11), 22597–22618. https://doi.org/10.1029/94JC01824

Brakstad, A., Våge, K., Håvik, L., & Moore, G. W. K. (2019). Water mass transformation in the Greenland Sea during the period 1986-2016. *Journal of Physical Oceanography*, *49*(1), 121–140. https://doi.org/10.1175/JPO-D-17-0273.1

Bringedal, C., Eldevik, T., Skagseth, Ø., Spall, M. A., & Østerhus, S. (2018). Structure and forcing of observed exchanges across the Greenland-Scotland ridge. *Journal of Climate*, *31*(24), 9881–9901. https://doi.org/10.1175/JCLI-D-17-0889.1

Budéus, G., Schneider, W., & Krause, G. (1998). Winter convective events and bottom water warming in the Greenland Sea. *Journal of Geophysical Research*, *103*(C9), 18513–18527. https://doi.org/10.1029/98JC01563

Chafik, L., & Rossby, T. (2019). Volume, heat, and freshwater divergences in the subpolar North Atlantic suggest the Nordic Seas as key to the state of the Mmeridional overturning circulation. *Geophysical Research Letters*, *46*(9), 4799–4808. https://doi.org/10.1029/2019GL082110

Chen, X., & Tung, K.-K. (2014). Varying planetary heat sink led to global-warming slowdown and acceleration. *Science*, *345*(6199), 897–903. http://doi.org/10.1126/science.1254937

Chen, X., & Tung, K.-K. (2018). Global surface warming enhanced by weak Atlantic overturning circulation. *Nature*, *559*(7714), 387–391. http://doi.org/10.1038/s41586-018-0320-y

de Steur, L., Hansen, E., Mauritzen, C., Beszczynska-Möller, A., & Fahrbach, E. (2014). Impact of recirculation on the East Greenland Current in Fram Strait: Results from moored current meter measurements between 1997 and 2009. *Deep Sea Research Part I: Oceanographic Research Papers*, *92*, 26–40. https://doi.org/10.1016/j.dsr.2014.05.018

Eldevik, T., Nilsen, J. E. Ø., Iovino, D., Anders Olsson, K., Sandø, A. B., & Drange, H. (2009). Observed sources and variability of Nordic Seas overflow. *Nature Geoscience*, *2*(6), 406–410. https://doi.org/10.1038/ngeo518

Fogelqvist, E., Blindheim, J., Tanhua, T., Østerhus, S., Buch, E., & Rey, F. (2003). Greenland-Scotland overflow studied by hydro-chemical multivariate analysis. *Deep Sea Research Part I: Oceanographic Research Papers*, *50*(1), 73–102. https://doi.org/10.1016/S0967-0637(02)00131-0

García-Ibáñez, M. I., Pérez, F. F., Lherminier, P., Zunino, P., Mercier, H., & Tréguer, P. (2018). Water mass distributions and transports for the 2014 GEOVIDE cruise in the North Atlantic. *Biogeosciences*, *15*(7), 2075–2090. https://doi.org/10.5194/bg-15-2075-2018

Good, S. A., Martin, M. J., & Rayner, N. A. (2013). EN4: Quality controlled ocean temperature and salinity profiles and monthly objective analyses with uncertainty estimates. *Journal of Geophysical Research: Oceans*, *118*(12), 6704–6716. https://doi.org/10.1002/2013JC009067

Hansen, B., Húsgarð Larsen, K. M., Hátún, H., Østerhus, S., & Østerhus, S. (2016). A stable Faroe Bank Channel overflow 1995-2015. *Ocean Science*, *12*(6), 1205–1220. https://doi.org/10.5194/os-12-1205-2016

Hansen, B., & Østerhus, S. (2000). North Atlantic-Nordic Seas exchanges. *Progress in Oceanography*, *45*(2), 109–208. https://doi.org/10.1016/S0079-6611(99)00052-X

Harden, B. E., Pickart, R. S., Valdimarsson, H., Våge, K., de Steur, L., Richards, C., et al. (2016). Upstream sources of the Denmark Strait overflow: Observations from a high-resolution mooring array. *Deep Sea Research Part I: Oceanographic Research Papers*, *112*, 94–112. https://doi.org/10.1016/j.dsr.2016.02.007

Hattermann, T., Isachsen, P. E., Appen, W. J., Albretsen, J., & Sundfjord, A. (2016). Eddy-driven recirculation of Atlantic Water in Fram Strait. *Geophysical Research Letters*, *43*(7), 3406–3414. https://doi.org/10.1002/2016GL068323

Håvik, L., Pickart, R. S., Våge, K., Torres, D., Thurnherr, A. M., Beszczynska-Möller, A., et al. (2017). Evolution of the East Greenland Current from Fram Strait to Denmark Strait: Synoptic measurements from summer 2012. *Journal of Geophysical Research: Oceans*, *122*(3), 1974–1994. https://doi.org/10.1002/2016JC012228

Hawker, E. J. (2005). *The Nordic Seas circulation and exchanges (Doctoral thesis)*. University of Southampton. Retrieved from University of Southampton Institutional Repository. http://eprints.soton.ac.uk/id/eprint/18669

Holliday, N. P., Hughes, S. L., Bacon, S., Beszczynska-Möller, A., Hansen, B., Lavín, A., et al. (2008). Reversal of the 1960s to 1990s freshening trend in the northeast North Atlantic and Nordic Seas. *Geophysical Research Letters*, *35*(3). https://doi.org/10.1029/2007GL032675

Huang, J., Pickart, R. S., Huang, R. X., Lin, P., Brakstad, A., & Xu, F. (2020). Sources and upstream pathways of the densest overflow water in the Nordic Seas. *Nature Communications*, *11*(1), 5389. http://doi.org/10.1038/s41467-020-19050-y

Jeansson, E., Jutterström, S., Rudels, B., Anderson, L. G., Anders Olsson, K., Jones, E. P., et al. (2008). Sources to the East Greenland Current and its contribution to the Denmark Strait overflow. *Progress in Oceanography*, *78*(1), 12–28. https://doi.org/10.1016/j.pocean.2007.08.031

Jeansson, E., Olsen, A., & Jutterström, S. (2017). Arctic intermediate water in the Nordic Seas, 1991-2009. *Deep Sea Research Part I: Oceanographic Research Papers*, *128*, 82–97. https://doi.org/10.1016/j.dsr.2017.08.013

Karstensen, J., Schlosser, P., Wallace, D. W. R., Bullister, J. L., & Blindheim, J. (2005). Water mass transformation in the Greenland Sea during the 1990s. *Journal of Geophysical Research: Oceans*, *110*(C7). http://doi.org/10.1029/2004JC002510

Köhl, A. (2010). Variable source regions of Denmark Strait and Faroe Bank Channel overflow waters. *Tellus A: Dynamic Meteorology and Oceanography*, *62*(4), 551–568. https://doi.org/10.1111/j.1600-0870.2010.00454.x

Kostianoy, A. G., & Nihoul, J. C. J. (2009). Frontal zones in the Norwegian, Greenland, Barents and Bering seas. In J. C. J. Nihoul, & A. G. Kostianoy, (Eds.), *Influence of climate change on the changing Arctic and sub-Arctic conditions* (pp. 171–190). Springer.

Langehaug, H. R., & Falck, E. (2012). Changes in the properties and distribution of the intermediate and deep waters in the Fram Strait. *Progress in Oceanography*, *96*(1), 57–76. https://doi.org/10.1016/j.pocean.2011.10.002

Latarius, K., & Quadfasel, D. (2016). Water mass transformation in the deep basins of the Nordic Seas: Analyses of heat and freshwater budgets. *Deep Sea Research Part I: Oceanographic Research Papers*, *114*, 23–42. https://doi.org/10.1016/j.dsr.2016.04.012

Lauvset, S. K., Brakstad, A., Våge, K., Olsen, A., Jeansson, E., & Mork, K. A. (2018). Continued warming, salinification and oxygenation of the Greenland Sea gyre. *Tellus A: Dynamic Meteorology and Oceanography*, *70*(1), 1–9. https://doi.org/10.1080/16000870.2018.1476434

Marnela, M., Rudels, B., Goszczko, I., Beszczynska-Möller, A., & Schauer, U. (2016). Fram Strait and Greenland Sea transports, water masses, and water mass transformations 1999-2010 (and beyond). *Journal of Geophysical Research: Oceans*, *121*(4), 2314–2346. https://doi.org/10.1002/2015JC011312

Marnela, M., Rudels, B., Houssais, M.-N., Beszczynska-Möller, A., & Eriksson, P. B. (2013). Recirculation in the Fram Strait and transports of water in and north of the Fram Strait derived from CTD data. *Ocean Science*, *9*(3), 499–519. https://doi.org/10.5194/os-9-499-2013

Marnela, M., Rudels, B., Olsson, K. A., Anderson, L. G., Jeansson, E., Torres, D. J., et al. (2008). Transports of Nordic Seas water masses and excess SF6 through Fram Strait to the Arctic Ocean. *Progress in Oceanography*, *78*(1), 1–11. https://doi.org/10.1016/j.pocean.2007.06.004

Mastropole, D., Pickart, R. S., Valdimarsson, H., Våge, K., Jochumsen, K., & Girton, J. (2017). On the hydrography of Denmark Strait. *Journal of Geophysical Research: Oceans*, *122*(1), 306–321. https://doi.org/10.1002/2016JC012007

McKenna, C., Berx, B., & Austin, W. E. N. (2016). The decomposition of the Faroe-Shetland Channel water masses using parametric optimum multi-parameter analysis. *Deep Sea Research Part I: Oceanographic Research Papers*, *107*, 9–21. https://doi.org/10.1016/j.dsr.2015.10.013

Merchel, M., & Walczowski, W. (2020). Increases in the temperature and salinity of deep and intermediate waters in the West Spitsbergen Current region in 1997-2016. *Oceanologia*, *62*(4 Part A), 501–510. https://doi.org/10.1016/j.oceano.2020.08.001

Moore, G. W. K., Våge, K., Pickart, R. S., & Renfrew, I. A. (2015). Decreasing intensity of open-ocean convection in the Greenland and Iceland seas. *Nature Climate Change*, *5*, 877. https://doi.org/10.1038/nclimate2688

Mork, K. A., Skagseth, Ø., Ivshin, V., Ozhigin, V., Hughes, S. L., & Valdimarsson, H. (2014). Advective and atmospheric forced changes in heat and fresh water content in the Norwegian Sea, 1951-2010. *Geophysical Research Letters*, *41*(17), 6221–6228. https://doi.org/10.1002/2014GL061038

Olsson, K. A., Jeansson, E., Anderson, L. G., Hansen, B., Eldevik, T., Kristiansen, R., et al. (2005). Intermediate water from the Greenland Sea in the Faroe Bank Channel: Spreading of released sulphur hexafluoride. *Deep Sea Research Part I: Oceanographic Research Papers*, *52*(2), 279–294. https://doi.org/10.1016/j.dsr.2004.09.009

Orvik, K. A., & Niiler, P. (2002). Major pathways of Atlantic water in the northern North Atlantic and Nordic Seas toward Arctic. *Geophysical Research Letters*, *29*(19), 1896. https://doi.org/10.1029/2002GL015002

Østerhus, S., & Gammelsrød, T. (1999). The abyss of the Nordic Seas is warming. *Journal of Climate*, *12*(11), 3297–3304. https://doi.org/10.1175/1520-0442(1999)012<3297:TAOTNS>2.0.CO;2

Østerhus, S., Woodgate, R., Valdimarsson, H., Turrell, B., de Steur, L., Quadfasel, D., et al. (2019). Arctic Mediterranean exchanges: A consistent volume budget and trends in transports from two decades of observations. *Ocean Science*, *15*(2), 379–399. https://doi.org/10.5194/os-15-379-2019

Pickart, R. S., Spall, M. A., Torres, D. J., Våge, K., Valdimarsson, H., Nobre, C., et al. (2017). The North Icelandic Jet and its relationship to the North Icelandic Irminger Current. *Journal of Marine Research*, *75*(5), 605–639. https://doi.org/10.1357/002224017822109505

Polyakov, I. V., Pnyushkov, A. V., Alkire, M. B., Ashik, I. M., Baumann, T. M., Carmack, E. C., et al. (2017). Greater role for Atlantic inflows on sea-ice loss in the Eurasian Basin of the Arctic Ocean. *Science*, *356*(6335), 285–291. http://doi.org/10.1126/science.aai8204

Richards, C. G., & Straneo, F. (2015). Observations of water mass transformation and eddies in the Lofoten Basin of the Nordic Seas. *Journal of Physical Oceanography*, *45*(6), 1735–1756. https://doi.org/10.1175/JPO-D-14-0238.1

Rossby, T., Prater, M. D., & Søiland, H. (2009). Pathways of inflow and dispersion of warm waters in the Nordic Seas. *Journal of Geophysical Research*, *114*(C4). https://doi.org/10.1029/2008JC005073

Rudels, B., Björk, G., Nilsson, J., Winsor, P., Lake, I., & Nohr, C. (2005). The interaction between waters from the Arctic Ocean and the Nordic Seas north of Fram Strait and along the East Greenland Current: Results from the Arctic Ocean-02 Oden expedition. *Journal of Marine Systems*, *55*(1–2), 1–30. https://doi.org/10.1016/j.jmarsys.2004.06.008

Rudels, B., Fahrbach, E., Meincke, J., Budéus, G., & Eriksson, P. (2002). The East Greenland Current and its contribution to the Denmark Strait overflow. *ICES Journal of Marine Science*, *59*(6), 1133–1154. https://doi.org/10.1006/jmsc.2002.1284

Rudels, B., Marnela, M., & Eriksson, P. (2008). Constraints on estimating mass, heat and freshwater transports in the Arctic Ocean: An exercise. In R. R. Dickson, J. Meincke, & P. Rhines (Eds.), *Arctic–subarctic ocean fluxes: Defining the role of the Northern Seas in climate* (pp. 315–341). Springer.

Schlichtholz, P., & Houssais, M.-N. (1999). An inverse modeling study in Fram Strait. Part II: Water mass distribution and transports. *Deep Sea Research Part II: Topical Studies in Oceanography*, *46*(6–7), 1137–1168. https://doi.org/10.1016/s0967-0645(99)00017-x

Schlichtholz, P., & Houssais, M.-N. (2002). An overview of the θ-S correlations in Fram Strait based on the MIZEX 84 data. *Oceanologia*, *44*(2), 243–272. https://doi.org/10.2134/jeq2003.1929

Schott, F., Visbeck, M., & Fischer, J. (1993). Observations of vertical currents and convection in the central Greenland Sea during the winter of 1988–1989. *Journal of Geophysical Research: Oceans*, *98*(C8). 14401–14421. https://doi.org/10.1029/93jc00658

Semper, S., Pickart, R. S., Våge, K., Larsen, K. M. H., Hátún, H., & Hansen, B. (2020). The Iceland-Faroe Slope Jet: A conduit for dense water toward the Faroe Bank Channel overflow. *Nature Communications*, *11*(1), 5390. http://doi.org/10.1038/s41467-020-19049-5

Shao, Q., Zhao, J., Drinkwater, K. F., Wang, X., & Cao, Y. (2019). Internal overflow in the Nordic Seas and the cold reservoir in the northern Norwegian Basin. *Deep Sea Research Part I: Oceanographic Research Papers*, *148*, 67–79. https://doi.org/10.1016/j.dsr.2019.04.012

Somavilla, R. (2019). Draining and upwelling of Greenland Sea deep waters. *Journal of Geophysical Research: Oceans*, *124*(4), 2842–2860. https://doi.org/10.1029/2018JC014249

Swift, J. H., & Aagaard, K. (1981). Seasonal transitions and water mass formation in the Iceland and Greenland seas. *Deep Sea Research Part A. Oceanographic Research Papers*, *28*(10), 1107–1129. https://doi.org/10.1016/0198-0149(81)90050-9

Swift, J. H., & Koltermann, K. P. (1988). The origin of Norwegian Sea deep water. *Journal of Geophysical Research*, *93*(C4), 3563–3569. https://doi.org/10.1029/JC093iC04p03563

Turrell, W. R., Slesser, G., Adams, R. D., Payne, R., & Gillibrand, P. A. (1999). Decadal variability in the composition of Faroe Shetland Channel bottom water. *Deep Sea Research Part I: Oceanographic Research Papers*, *46*(1), 1–25. https://doi.org/10.1016/S0967-0637(98)00067-3

Våge, K., Moore, G. W. K., Jónsson, S., & Valdimarsson, H. (2015). Water mass transformation in the Iceland Sea. *Deep Sea Research Part I: Oceanographic Research Papers*, *101*, 98–109. https://doi.org/10.1016/j.dsr.2015.04.001

Våge, K., Pickart, R. S., Spall, M. A., Moore, G. W. K., Valdimarsson, H., Torres, D. J., et al. (2013). Revised circulation scheme north of the Denmark Strait. *Deep Sea Research Part I: Oceanographic Research Papers*, *79*, 20–39. https://doi.org/10.1016/j.dsr.2013.05.007

Våge, K., Pickart, R. S., Spall, M. A., Valdimarsson, H., Jónsson, S., Torres, D. J., et al. (2011). Significant role of the North Icelandic Jet in the formation of Denmark Strait overflow water. *Nature Geoscience*, *4*(10), 723–727. https://doi.org/10.1038/ngeo1234

Visbeck, M., & Rhein, M. (2000). Is bottom boundary layer mixing slowly ventilating Greenland Sea deep water. *Journal of Physical Oceanography*, *30*(1), 215–224. http://doi.org/10.1175/1520-0485(2000)030<0215:IBBLMS>2.0.CO;2

Voet, G., Quadfasel, D., Mork, K. A., & Søiland, H. (2010). The mid-depth circulation of the Nordic Seas derived from profiling float observations. *Tellus A: Dynamic Meteorology and Oceanography*, *62*(4), 516–529. https://doi.org/10.1111/j.1600-0870.2010.00444.x

Wang, X., Zhao, J., Li, T., Zhong, W., & Jiao, Y. (2015). Deep waters warming in the Nordic seas from 1972 to 2013. *Acta Oceanologica Sinica*, *34*(3), 18–24. http://doi.org/10.1007/s13131-015-0613-z

Yashayaev, I., & Seidov, D. (2015). The role of the Atlantic Water in multidecadal ocean variability in the Nordic and Barents Seas. *Progress in Oceanography*, *132*, 68–127. https://doi.org/10.1016/j.pocean.2014.11.009